REMOVAL OF THE PHASE NOISE IN THE AUTOCORRELATION ESTIMATES WITH DATA WINDOWING

Mustafa A. Altınkaya[1], Emin Anarım[2] and Bülent Sankur[2]

[1] Department of Electrical & Electronics Engineering,
İzmir Institute of Technology, İzmir, Türkiye
phone: + (90) 232 750 6529, fax: + (90) 232 750 6505,
email: mustafaaltinkaya@iyte.edu.tr,
web: www.iyte.edu.tr/~mustafaaltinkaya

[2] Department of Electrical & Electronics Engineering,
Boğaziçi University, İstanbul, Türkiye
phone: + (90) 212 359 6414, fax: + (90) 212 2872465,
email: {anarim, sankur}@boun.edu.tr
web: busim.ee.boun.edu.tr/{academic/~anarim, ~sankur}

ABSTRACT

The sinusoidal frequency estimation from short data records based on Toeplitz autocorrelation (AC) matrix estimates suffer from phase noise. This effect becomes prominent especially when additive noise vanishes becoming a nuisance, that is at high signal-to-noise ratios (SNR). Based on both analytic derivation of the AC lag terms and simulation experiments, we show that data windowing can mitigate the limitations caused by the phase noise. Thus with proper windowing, the variance of the frequency estimate is no more limited by phase noise, but it continues to decrease linearly with the SNR. The cases of the Pisarenko frequency estimator and of MUSIC, both for the single sinusoid case, are analyzed in detail.

1. INTRODUCTION

The problem of sinusoidal frequency estimation in an additive noise environment is a commonly encountered problem in such diversive areas as communication systems, geophysics, vibration analysis, acoustics and biomedical applications. Although the maximum likelihood method gives the theoretically best performance, it requires to solve nonlinear optimization problems in the case of closely spaced sinusoids in the frequency. So, model-based suboptimum techniques has been used extensively due to their computational advantages and high resolution property. Especially, when the data record has a limited number of samples, model-based spectral estimation techniques show superior performance in general. Many of these techniques use autocorrelation (AC) lags of the data in order to estimate the frequencies of the sinusoids. In this work, we consider two subspace-based methods which utilize the Toeplitz AC matrix estimate to find the sinusoidal frequencies.

An important disadvantage in the utilization of the Toeplitz AC matrix for the frequency estimation with short data records is the observation of a minimum attainable variance of the estimators even when the signal-to-noise ratio (SNR) is increased unboundedly. This error floor effect is caused by the phase noise. The data windowing is shown to mitigate this handicap which is the main contribution of this paper.

In section 2. the sinusoidal frequency estimation problem and the utilized frequency estimators, namely, Pisarenko frequency estimator (PISFE) and Multiple Signal Characterization (or Classification) (MUSIC) are defined. In Section 3. the statistics of the AC lag estimates with and without data windowing are derived. In Section 4. the probability density function (pdf) of PISFE with and without data windowing is derived and performance improvement caused by the data windowing is shown based on both analytical and experimental results. Section 5 covers the simulation results of MUSIC and PISFE showing the elimination of the variance lower bound on the frequency estimates by data windowing. Finally, the conclusions are given in Section 6. Detailed derivation of the pdf of AC lags with data windowing is given in the appendix in order to make the paper easier to follow.

2. FREQUENCY ESTIMATION PROBLEM AND UTILIZED MODEL-BASED ESTIMATORS

The signal model under consideration consists of multiple real sinusoids observed in additive white Gaussian noise (AWGN), i.e.,

$$x_k = \sum_{i=1}^{K} \sqrt{2A_i} \cos[\omega_i kT + \phi_i] + n_k \quad k = 1, 2, ...N$$

where A_i, ϕ_i and ω_i are the non-random amplitude, the random phase angle uniformly distributed on $(-\pi, \pi)$ and the angular tone frequency of the ith real sinusoid, respectively, and T is the sampling period, $\{n_k\}$ is a real white Gaussian noise sample sequence with zero mean and power σ_n^2 and N is the number of data samples. We are interested only in the angular frequency parameter. The other parameters are considered as nuisance parameters. We assume without loosing generality that the number of the sinusoids is either known or can be estimated from the data. We also drop the index of the sinusoidal parameters for the single sinusoid case. The results of the data windowing which are developed in this paper are also valid for the more useful multiple sinusoids case, but we preferred in this paper to use a single sinusoid case to emphasize the main points of the work. In this work we use two different frequency estimators, namely, PISFE and MUSIC frequency estimators which we will define briefly.

For a single sinusoid case, PISFE is obtained in terms of the AC coefficients by assuming $T = 1$ as follows [1]:

$$\hat{\omega} = \arccos(\psi) \tag{1}$$

where

$$\psi = \frac{r(2) + \sqrt{r^2(2) + 8r^2(1)}}{4r(1)}$$

and $r(k)$ denotes the kth autocorrelation coefficient of the input samples and is calculated as $r(k) = \left(\sum_{i=1}^{N-k} x_i x_{i+k} \right) / (N-k)$ which shows that the estimated tone frequency depends on the AC coefficient at lags 1 and 2, and does not depend on the signal waveform. For a single tone case, this result is very practical for its computational simplicity.

PISFE is a special case of the more general MUSIC frequency estimator. To obtain the MUSIC frequency estimator first the Toeplitz sample estimate of the $M \times M$ AC matrix is built as $\{R_M(i, j) = r(|i - j|), i, j = 1, ..., M\}$. The MUSIC power spectrum is given as:

$$\text{MUSIC}(f) = \frac{1}{\sum_{k=2K+1}^{M} |\mathbf{p}^\dagger(f)\mathbf{v}_k|^2}$$

where the set $\{\mathbf{v}_i, i = 2K + 1, ..., M\}$ contains the M-dimensional noise subspace eigenvectors corresponding to the $M - 2K$ smallest eigenvalues of the AC matrix estimate and $\mathbf{p}^\dagger(f) = [1 \ e^{-j2\pi f} \ \cdots \ e^{-j2\pi(M-1)f}]$. The estimated tone frequency (or frequencies) is (are) found by picking the K peak-pairs of this power spectrum which correspond to K real tones.
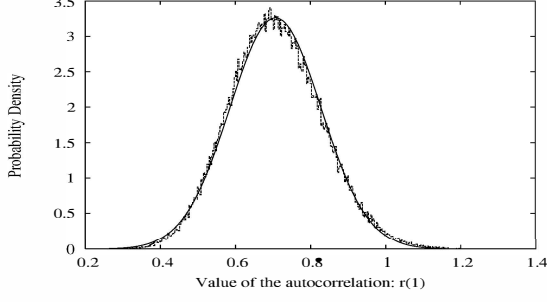
Figure 1: Pdf of $r_x(1)$: **low SNR case**, solid line: analytic computation, histogram lines: histogram obtained by simulation ($\omega = \pi/4$ (rad), $N = 50$, SNR = 5 dB, 100 000 noise realizations.)
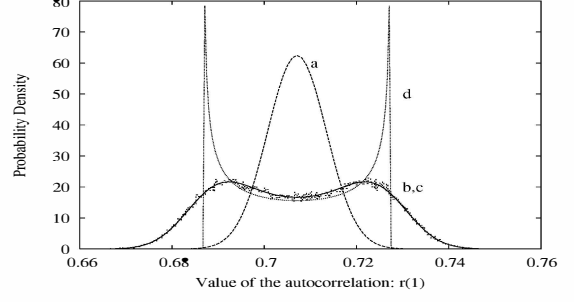

Figure 2: Pdf of $r_x(1)$: **high SNR case**, a: pdf of $r_{x,g}(1)$ (only Gaussian component, analytic computation),b: pdf of $r_x(1)$ (analytic computation), c: histogram obtained by simulation, d: pdf of $(r_{x,h}(1) + \cos(\omega))$ (shifted phase noise component, analytic computation) ($\omega = \pi/4$ (rad), $N = 50$, SNR = 30 dB, 100 000 noise realizations.)

3. THE NEED FOR DATA WINDOWING

In order to find the performance of the frequency estimators based on the Toeplitz AC matrix estimate, the statistics of the sample AC coefficients must be derived. For a single sinusoid of angular frequency ω the AC lag estimates are given by

$$
\begin{aligned}
r_x(l) &= \frac{1}{N-l}\sum_{k=1}^{N-l}\Big\{ A[\cos(\omega lT) + \cos(\omega(2k+l)T + 2\phi)] \\
&\quad + \left(\sqrt{2A}\cos(\omega kT + \phi)n_{k+l}\right) \\
&\quad + \left(\sqrt{2A}\cos(\omega(k+l)T + \phi)n_k\right) + n_k n_{k+l}\Big\}.
\end{aligned}
$$

The large sample statistics of $r_x(l)$ was derived in [2] where it is shown to be Gaussian distributed with mean and variance

$$
\mu_x(l) = A\cos(\omega lT) \qquad \text{for } i = 1,\ldots,N-1 \tag{2}
$$

$$
c_x(l) = \frac{\sigma_n^4}{N}(1 + 4A/\sigma_n^2\cos^2(\omega lT)) \quad \text{for } i = 1,\ldots N-1 \tag{3}
$$

respectively. For more practical small sample sizes let us express $r_x(l)$ as

$$
r_x(l) = r_{x,h}(l) + r_{x,g}(l) \tag{4}
$$

where

$$
r_{x,h}(l) = \frac{1}{N-l}\sum_{k=1}^{N-l}A\cos(\omega(2k+l)T + 2\phi)
$$

and $r_{x,g}(l)$ corresponds to the sum of all the remaining terms in (4) which have AWGN terms inside and the deterministic component $A\cos(\omega lT)$. In this study, we neglect the dependence of $r_{x,h}(l)$ and $r_{x,g}(l)$ and derive the pdf of $r_x(l)$ under the assumption that they are statistically independent. The comparison of the derived analytical pdf expressions with histograms obtained by simulation experiments show that there is not any considerable loss due to the commited approximation. So, (4) is a sum of two independent random variables. The pdf of this quantity can be obtained as a convolution of the pdfs of the two random variables. One can easily obtain the pdf of $r_{x,h}(l)$ as

$$
f_{R_{x,h}}^{(l)}(r_{x,h}) = \frac{1}{\pi d(l)\sqrt{1 - (r_{x,h}(l)/d(l))^2}} \quad \text{for } -d(l) < \omega < d(l). \tag{5}
$$

This pdf has the form of the derivative of the arcsin ω scaled with the constant $d(l)$ which can be found using a rectangular window in (10). Notice that for large sample sizes $r_{x,h}(l)$ will tend to zero. Here, we make an assumption that $r_{x,g}(l)$ will also have approximately the Gaussian distribution valid for the large sample case with mean $\mu_x(l)$ and variance $c_x(l)$. So, the pdf of $r_x(l)$ is found as the result of the convolution

$$
f_{R_x}^{(l)}(r_x) = \int_{-d(l)}^{d(l)} \frac{\exp\left\{-\frac{1}{2}\frac{(r_x(l)-\tau-\mu_x(l))^2}{c_x(l)}\right\}}{\pi d(l)\sqrt{1 - (\tau/d)^2}\sqrt{2\pi c_x(l)}} d\tau. \tag{6}
$$

In Figures 1 and 2 we plotted the pdf of $r_x(1)$ together with the histogram obtained as a result of simulations with 100,000 independent runs of a single sinusoid in AWGN where $\omega = \pi/4$ and $N = 50$. In Figure 1, SNR = 5 dB whereas it is 30 dB in Figure 2. In Figure 1, we observe close matching of the histogram and the pdf calculated as a Gaussian waveform with mean $\mu_x(1)$ and variance $c_x(1)$ corresponding to the large sample size case. For this *low* SNR value of 5 dB also the pdf computed using (6) perfectly matches the plotted Gaussian pdf. For a *high* SNR value of 30 dB the pdf of $r_x(1)$ no longer resembles a Gaussian waveform as it is depicted in Figure 2. In fact, its shape is governed by the pdf of the phase dependent term $r_{x,h}(1)$ since the frequency interval for which this term is non-zero is constant independent of the SNR. This behavior makes it impossible for the variance of the AC lag estimates to tend to zero as the SNR increases unboundedly. On the contrary, an asymptotic lower bound exists which is given by the variance of the $r_{x,h}(l)$. This behavior will also cause an error floor on the variance of the frequency estimates obtained using estimators based on these AC lags. The pdf of $r_x(1)$ computed by (6) and the simulation histogram again match closely. In this figure also the pdfs of the individual Gaussian and phase noise components are plotted, which are computed again as a Gaussian pdf corresponding to the large sample size case and using (5) with $l = 1$, respectively.

We suggest data windowing to prevent this unwanted large SNR behavior of such estimators. Remembering the Wiener-Khinchine relationship between the AC lags and the power spectrum, one can intuitively think of eliminating the leakage in the AC lags with data windowing just like it is the case in DFT analysis based methods. The data windowing is hoped to decrease the frequency interval where the pdf of the phase dependent term is non-zero.

The statistics of the AC lags after data windowing are obtained in Appendix A. These estimates, namely, $r_{y,h}(l)$ and $r_{y,g}(l)$ again have pdf's of the same form as the ones of $r_{x,h}(l)$ and $r_{x,g}(l)$, respectively. However due to the rôle of data windowing in reducing the interval where $f_{R_{y,h}}^{(l)}(r_{y,h})$ is nonzero, their convolution is now approximately Gaussian even at high SNRs. We will demonstrate this by comparing the simulation histograms and the pdf expressions of PISFE under Gaussianity assumption of the AC lags.

4. THE PDF OF PISFE

The pdf of PISFE, $\hat{\omega}$, is obtained from the pdf of the intermediate random variable ψ using the transformation

$$
f_{\text{PISFE}}(\hat{\omega}) = \sqrt{1 - \cos^2(\hat{\omega})}f_\psi(\cos\hat{\omega}). \tag{7}
$$

We will present the derivation of the pdf of ψ elsewhere due to space limitation. The derivations are based on the Central Limit Theorem
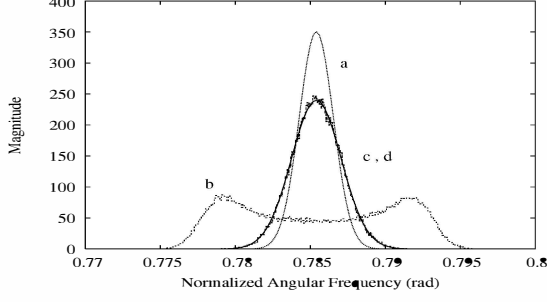
Figure 3: Pdf of PISFE with and without data windowing versus normalized angular frequency, a: analytic computation for non-windowed data, b: histogram for non-windowed data simulation, c: analytic computation for windowed data, d: histogram for windowed data simulation ($\omega = \pi/4$ (rad), $N = 100$, SNR = 20 dB, data window: Blackman-Harris type window of Nuttall with coefficients, $a_0 = 10/32$, $a_1 = 15/32$, $a_2 = 6/32$, $a_3 = 1/32$).

Figure 4: Variance of the PISFE and MUSIC frequency estimates with and without data windowing versus SNR, a: PISFE , b: PISFE (with data windowing), c: MUSIC, d: MUSIC (with data windowing) ($\omega = 0.5$ (rad), $N = 50$, data window: Blackman-Harris type window of Nuttall with coefficients, $a_0 = 10/32$, $a_1 = 15/32$, $a_2 = 6/32$, $a_3 = 1/32$).

(CLT) so the pdf expression is expected to be valid only for large N (e.g. $N \geq 50$). The pdf is

$$f(\psi) = \frac{4K_1 e^{\frac{-A_4}{2}}}{A_2(\psi)} \left[\frac{B_1(\psi)u(\psi)}{(1 + A_1(\psi))} + \frac{B_2(\psi)u(-\psi)}{(1 - A_1(\psi))} \right] \quad (8)$$

where $u(\cdot)$ represents the unit step function. The remaining definitions are given as:

$$K_1 = \frac{1}{2\pi\sigma_1\sigma_2\sqrt{1-\rho^2}}$$

$$A_0(\psi) = (2\psi^2 - 1)/\psi$$

$$A_1(\psi) = A_0(\psi)/\sqrt{A_0^2(\psi) + 8}$$

$$A_2(\psi) = \frac{1}{(1-\rho^2)} \left[\left(\frac{A_0(\psi)}{\sigma_2} \right)^2 + \frac{1}{\sigma_1^2} - \frac{2\rho A_\bullet(\psi)}{\sigma_1\sigma_2} \right]$$

$$A_3(\psi) = \frac{2}{(1-\rho^2)} \left[\frac{\rho}{\sigma_1\sigma_2}(\mu(2) + A_\bullet(\psi)\mu(1)) - \frac{\mu(1)}{\sigma_1^2} - \frac{A_\bullet(\psi)\mu(2)}{\sigma_2^2} \right]$$

$$A_4 = \frac{1}{(1-\rho^2)} \left[\left(\frac{\mu(1)}{\sigma_1} \right)^2 + \left(\frac{\mu(2)}{\sigma_2} \right)^2 - \frac{2\rho\mu(1)\mu(2)}{\sigma_1\sigma_2} \right]$$

$$B_1(\psi) = \left[1 + \frac{A_3(\psi)}{4}\sqrt{\frac{2\pi}{A_2(\psi)}} \exp\frac{A_3^2(\psi)}{8A_2(\psi)} \left(\text{erf}\left(\frac{A_3(\psi)}{\sqrt{8A_2(\psi)}} \right) - 1 \right) \right]$$

$$B_2(\psi) = \left[1 + \frac{A_3(\psi)}{4}\sqrt{\frac{2\pi}{A_2(\psi)}} \exp\frac{A_3^2(\psi)}{8A_2(\psi)} \left(\text{erf}\left(\frac{A_3(\psi)}{\sqrt{8A_2(\psi)}} \right) + 1 \right) \right]$$

with $\{\mu(i), i = 1, 2\}$ and $\{\sigma_1^2 = c(i), i = 1, 2\}$ representing the means and variances of the first two AC lags given by (2) and (3), respectively, and $\rho = \text{cov}(r(1), r(2))/(c(1)c(2))^{1/2}$ is their correlation coefficient where

$$\text{cov}(r(1), r(2)) = \left[\frac{4A\sigma_n^2}{N} \right] \cos(\omega T)\cos(2\omega T) \quad (9)$$

is their cross-covariance. Finally, $\text{erf}(\cdot)$ denotes the error function.

We performed simulations with and without data windowing and also calculated the corresponding pdf using (7) and (8). In the calculation of the pdf of PISFE, the pdf of the AC lags are modeled by the Gaussian densities with means and covariances defined by (2), (3) and (9) for the non-windowed data and by (11), (14) and (13) for the windowed data, respectively. The normalized angular frequency $\omega = \pi/4$ (rad), the sample size $N = 100$ and the number of the independent runs in the simulation is 100,000. The results
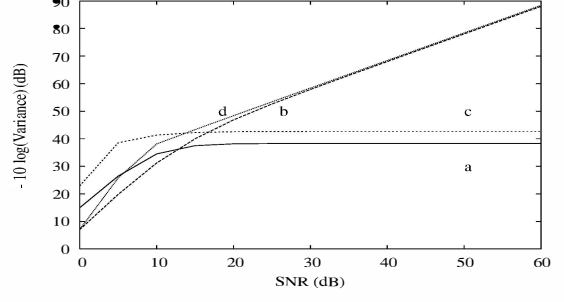
in Figure 3 depict that without data windowing the statistics of the AC lags are different from the pdfs in [2] even at this not very high SNR of 20 dB which is evident from the mismatch of the analytical computation of the pdf and the histogram of the simulation results. On the other hand, when a data window is utilized, the analytically computed pdf and the histogram perfectly matches. When the computed pdfs with and without data windowing are compared, one can see a performance degradation introduced by the data window since the width of the pdf is increased. However, one should consider that the computed pdf with no data window belongs to a *clairvoyant* estimator which does not exist. In other words, the Gaussianity assumption on the pdfs of the AC lag estimates fails which in turn makes the pdf expression of PISFE based on this assumption invalid.

We used a Blackman-Harris type data window with continuous fifth order derivatives [3] which showed good performance when compared with other windows in terms of the introduced bias and variance and also eliminated the splitting of the pdf.

5. EFFECTS OF DATA WINDOWING ON THE VARIANCE OF PISFE AND MUSIC FREQUENCY ESTIMATES

We also performed simulations to demonstrate the variance floor of the considered frequency estimators which utilize the Toeplitz AC matrix estimate. In Figure 4 we plotted the variance of the PISFE and MUSIC frequency estimates with and without data windowing. The curves are obtained by averaging the results of 10,000 independent runs where $\omega = 0.5$ (rad) and $N = 50$. The data window is again the same Blackman-Harris type window as the one used for the previous figure. The AC matrix is 10×10 for the MUSIC estimator. Without data windowing an error floor of - 38 dB and - 43 dB is observed for PISFE and MUSIC, respectively. The utilization of the data windowing cancels this behavior as it is depicted in the related variance curves of PISFE and MUSIC. At low SNR values the phase noise is ineffective and a performance loss in the variance figures are observed due to the property of data windowing to reduce the resolution capability of the frequency estimators. The increase in variance due to the data windowing at SNR = 0 dB, is about 8 dB and 14 dB for PISFE and MUSIC, respectively. As the SNR gets higher, the gain due to the eliminated phase noise increases and approximately at SNR = 13 dB it compensates the loss due to the decreased resolution. Increasing the SNR further, increases the variance reduction due to the data windowing which is 45 dB and 49 dB for MUSIC and PISFE, respectively, at SNR = 60 dB. The results of this simulation are valid for any ω with possible exceptions of some particular frequencies of the specific frequency estimator which are robust to the phase noise [4, 5].

6. CONCLUSIONS

In this study we considered the phase noise problem in sinusoidal frequency estimation using Toeplitz AC matrix estimates for small sample sizes. Our contributions can be listed as follows:

- We showed that the pdfs of AC estimates result from the convolution of the Gaussian pdf for the large sample size case and a double peaked pdf due to the random phase of the sinusoid which is a scaled derivative of the inverse sine function. We demonstrated the validity of our claims comparing our analytical results with simulation histograms both at low SNRs and at high SNRs where the pdf becomes governed by the phase noise.

- We suggested data windowing to eliminate the effects of the phase noise and derived the pdfs of the windowed AC estimates for the windowed data.

- In order to illustrate the corresponding benefit for the frequency estimators due to data windowing we considered applying PISFE to estimating the frequency of the single sinusoid in AWGN. We showed the phase noise governed behavior of the pdf of PISFE at high SNRs with simulation histograms. We gave an analytical expression for this pdf under Gaussianity of the AC estimates assumption with and without data windowing. This pdf was shown to closely match the simulation histogram as a consequence of the success of the data windowing in eliminating the phase noise disturbance.

We conclude that in the given problem the frequency estimation quality becomes governed by the phase noise at high SNRs and data windowing prevents this by making the AC estimates, and in turn the frequency estimators using them, have increasingly narrower pdfs as the SNR gets higher while the cost is the increased variance at low SNR values due to the reduction in the resolution capability of the estimators.

The windowing functions should be selected in a way to make a compromise between the amount of decrease in the resolution capability and the sidelobe reduction ability. We found that continuous fifth order derivatives at the borders, produced satisfactory windowing performance.

Our results on the elimination of the phase noise with data windowing is valid for any frequency estimator based on the Toeplitz AC matrix estimate. However, model-based frequency estimators of high subspace dimensions like MUSIC generally utilize AC matrix estimates constructed using the so called *covariance method* [6] which does not suffer from the phase noise. Consequently, the proposed data windowing is practically useful for the frequency estimators which inherently utilize the Toeplitz AC matrix estimate like Pisarenko harmonic decomposition and Yule-Walker method with Levinson-Durbin recursion. In spite of their inferior performance these frequency estimators are computationally very advantageous due to the Toeplitz structure and without the proposed data windowing we think that they are essentially incompletely defined.

As a final conclusion we advise to use data windowing with frequency estimators which are inherently based on Toeplitz AC matrix estimate in order to be able to obtain frequency estimates with variances smaller than the variance lower bound given by the phase noise. If this lower bound corresponds to an accuracy more than the requirement, data windowing should not be applied prior to the frequency estimation in order not to decrease the frequency resolution.

We should also say that we could not give the derivation of the PISFE pdf, performance comparisons with other estimators and considerations of choosing the data window in this paper due to space limitation. Those will be given elsewhere.

A. PDF OF THE AC-LAGS AFTER DATA WINDOWING

Let $y_k = w_k x_k$ where $\{w_k, k = 1, 2, \ldots, N\}$ represents a data window [3]. For a rectangular window function the asymptotic pdf of $r_y(i) = r_x(i) = r_{x,h}(i) + r_{x,g}(i)$ is the convolution of the pdf's of $r_{x,h}(i)$ and $r_{x,g}(i)$ referred to as $f_{R_{x,h}}^{(i)}(r_{x,h})$ and $f_{R_{x,g}}^{(i)}(r_{x,g})$, respectively.

$f_{R_{x,h}}^{(i)}(r_{x,h})$ has the form in (5) and $f_{R_{x,g}}^{(i)}(r_{x,g})$ was found to be Gaussian [2]. It can be shown easily that $f_{R_y}^{(i)}(r_y) = f_{R_{y,h}}^{(i)}(r_{y,h}) * f_{R_{y,g}}^{(i)}(r_{y,g})$ where $r_y(i) = r_{y,h}(i) + r_{y,g}(i)$. In the case of a general data window $f_{R_{y,h}}^{(i)}(r_{y,h})$ again has the form of (5), but now $d(i)$ is given by:

$$d(i) = \frac{1}{N-i} \left(\sum_{k=1}^{N-i} \sum_{l=1}^{N-i} w_k w_{k+i} w_l w_{l+i} \cos(\omega(k-i)) \right)^{1/2}. \quad (10)$$

The distribution of $r_{y,g}(i)$'s are again Gaussian due to the CLT but their first and second moments are affected by the windowing function. Now these moments are derived where the derivation closely follows the derivation in [2] for the non-windowed data.

The mean of the $r_y(i)$ is:

$$\mu_{y,g}(i) = \frac{1}{N-i} \sum_{k=1}^{N-i} w_k w_{k+i} \mu_{x,g}(i) \quad (11)$$

where $\mu_{x,g}(i) = E\{r_{x,g}(i)\} = A\cos(\omega i T) + \sigma_n^2 \delta_{i,j}$ with $\delta_{i,j}$ denoting the Kronecker delta which equals either unity in the case of $i = j$ or zero for the other cases. So, the covariance of $r_{y,g}(i)$ and $r_{y,g}(j)$ can be calculated as

$$c_{y,g}(i,j) = \frac{1}{(N-i)(N-j)} \sum_{k=1}^{N-i} \sum_{l=1}^{N-j} w_k w_{k+i} w_l w_{l+i} \quad (12)$$
$$E\{((s_k + n_k)(s_{k+i} + n_{k+i}) - \mu_{x,g}(i))$$
$$((s_l + n_l)(s_{l+i} + n_{l+i}) - \mu_{x,g}(j))\}.$$

After tedious steps one obtains

$$c_{y,g}(i,j) = \frac{\sigma_n^2}{(N-i)(N-j)} \sum_{k=1}^{N-i} \sum_{l=1}^{N-j} (w_k w_{k+i} w_l w_{l+i}) \quad (13)$$
$$\{\mu_s(k-l)\delta_{k+i,l+j} + \mu_s(k-(l+j))\delta_{k+i,l}$$
$$+ \mu_s((k+i)-l)\delta_{k,l+j} + \mu_s((k+i)-(l+j))\delta_{k+i,l+j}$$
$$+ \sigma_n^2 [\delta_{k,l}\delta_{k+i,l+j} + \delta_{k,k+i}\delta_{l,l+j}$$
$$+ \delta_{k,l+j}\delta_{l,k+i} + \delta_{i,0}\delta_{j,0}]\}.$$

When $i = j$, (13) simplifies to

$$c_{y,g}(i,i) = \frac{\sigma_n^2}{(N-i)^2} \left\{ \sum_{k=1}^{N-i} 2A w_k^2 w_{k+i}^2 + \sum_{k=1}^{N-2i} 2A\cos(2i\omega T) \right.$$
$$\left. w_k w_{k+i}^2 w_{k+2i} + \sigma_n^2 \sum_{k=1}^{N-i} w_k^2 w_{k+i}^2 \right\}. \quad (14)$$

REFERENCES

[1] Y.F.Pisarenko, "The Retrieval of Harmonics from a Covariance Function", Geophy. J.R. Astr. Soc., Vol.33, Jan. 1973, pp. 347-366.

[2] P. Stoica, T. Söderström and F.-N. Ti, "Overdetermined Yule-Walker Estimation of the Frequencies of Multiple Sinusoids: Accuracy Aspects", Signal Processing, Vol. 16, 1989, pp. 155-174.

[3] A. H. Nuttall, "Some Windows with Very Good Sidelobe Behavior", IEEE Trans. on Acoust. Speech, Signal Processing, Vol. ASSP-29, No. 1, Feb. 1981, pp. 84-91.

[4] K.W. Chan and H.C. So, "An Exact Analysis of Pisarenko's single-tone frequency estimation algorithm", Signal Processing, Vol. 83, No. 3, Mar. 2003, pp. 685-690.

[5] H. Sakai, "Statistical Analysis of Pisarenko's Method for Sinusoidal Frequency Estimation", IEEE Trans. on Acoust. Speech, Signal Processing, Vol. ASSP-32, No. 1, Feb. 1984, pp. 95-101.

[6] S.M. Kay, Modern spectral estimation: theory and application, Prentice Hall, New Jersey, 1988.